

3655

In-vivo phase imaging of growing epiphyseal human cartilage at 7 T.

Barbara Dymerska¹, Klaus Bohndorf¹, Paul Schennach¹, Alexander Rauscher², Siegfried Trattnig¹, and Simon Daniel Robinson¹

¹High Field MR Centre, Department of Biomedical Imaging and Image-guided Therapy, Medical University of Vienna, Vienna, Austria, ²UBC MRI Research Centre, University of British Columbia, Vancouver, Canada

Synopsis

Growing epiphyseal cartilage of children contains vessels and more complex layer structure than adult hyaline cartilage. Phase imaging is sensitive to deoxyhemoglobin in venous blood and to orientation of magnetic tissues, but it is challenging since many established methods for combining and unwrapping data fail in the thin cartilage of the knee. In this study different phase reconstruction methods were tested at 7T and high resolution SWI was applied to visualize veins and collagen fiber architecture in healthy young subjects.

Introduction

In contrast to adult hyaline cartilage, growing epiphyseal cartilage of children and adolescents contains vessels and more complex layer structure. Inroads towards establishing cartilage vessel imaging in animals and juvenile humans ex-vivo have been made recently¹⁻⁴. In vivo, phase imaging in knee cartilage is challenging since many established methods for combining and unwrapping data fail in thin, disconnected tissue regions and in children measurement times must be kept very short. In this study SWI was applied to exploit the sensitivity of the MR phase to deoxyhemoglobin in venous blood. The phase signal is also dependent on the orientation of magnetic tissues with respect to B_0 , making it sensitive to the architecture of cartilage fibers⁵. We present here the comparison of different phase reconstruction methods and first in-vivo SWI results at 7T in healthy young subjects with a focus on vein and collagen fiber architecture.

Methods

Six children participated in this study with the written informed consent of their legal guardians: C1–C6 with age = (6, 10, 10, 10, 13, 15) y.o..

Measurements were performed with a 7T Siemens Magnetom scanner and a 28 channel knee coil (QED).

Target scan: 3D gradient-echo sagittal acquisition with TE/TR=10.3 ms/23 ms, receiver bandwidth RBW=140 Hz/pixel, flip angle 9°, 448×{308,308,322,392,434}×88 matrix sizes (with the adjustment in phase encoding direction to subject-specific FOV), 0.3 mm in-plane resolution and between 1.0 mm and 1.4 mm thick slices, acquisition time (TA) between 3 min 8 sec and 4 min 14 sec.

Reference scan: 3D short echo-time gradient-echo scan acquired for the phase reconstruction with COMPOSER⁶ with vTE/TR=0.8 ms/14 ms, RBW=400 Hz/pixel, flip angle 4°, matrix size 128×64×40, 1.8×1.8×2.3 mm³ resolution, and TA=25 s.

The separate-channel target phase was combined using several reconstruction methods: MCPC-C⁷, VRC⁸, COMPOSER⁶, PRELUDE unwrap-and-filter⁹, Laplace unwrap-and-filter¹⁰, and Homodyne filter¹¹. The reconstruction quality was assessed by visual inspection of the combined phase and by the phase matching quality index, $Q^{6,12}$. $Q \approx 100\%$ denotes optimal phase matching, $Q \approx 0\%$ represents poor matching and high noise.

Phase combined using COMPOSER was Laplace unwrapped, high-pass filtered and a positive phase mask was created, which was multiplied with the magnitude data creating SWI for the visualization of veins and cartilage layers.

Results

Figure 1 presents combined phase and Q-maps for the subject with the thinnest cartilage (C6), for whom data combination was the most challenging. MCPC-C yielded reasonable phase matching in the cartilage close to the center of the image ($Q \approx 95\%$), but reduced values away from it (e.g. $Q = 80\%$ at the arrow position), where phase became more noisy. In PRELUDE unwrap-and-filter approach separate-channel phase was corrupted by multitude unwrapping errors, which strongly influenced the quality of the combined phase in the whole cartilage ($Q \approx 30\%$). Laplace unwrap-and filter method yielded Q-values between 90%-99% (with lowest value at arrow position). In Homodyne filtered images, $Q \approx 99\%$ was in the whole cartilage except for in a narrow region where a sudden drop occurred and open-ended fringe line was observed (see arrow). The best phase matching results were observed for VRC and COMPOSER methods with $Q \approx 99\%$, low noise, good contrast in the combined phase and no artifacts.

In **Figure 2** examples of vein appearance in SWI in the growing cartilage at different developmental stages are shown. Dot-like structures represent vessels perpendicular to the imaging plane, linear structures correspond to veins parallel to the imaging plane (see arrows). A variability in the cartilage thickness and vessel density was observed in subjects with age 10 (C2, C3 and C4). The vessel network in subject C3 is more similar to C1 (age 6) and in C2 more alike to C5 (age 13). The trend of diminishing vessel networks with age is, however, apparent when investigating the images from the youngest to the oldest child. In the latter (C6, age 15) no vessels were visible.

Contrast gained in SWI originating from different fiber orientations in the cartilage is presented in **Figure 3**. Hypo-intense regions are assumed to correspond to organized fiber structures (tangential or radial zones) and hyper-intense to isotropic regions⁵. In magnitude-only images these cartilage layers with different fiber orientation are undistinguishable.

Discussion and conclusions

This is the first study of growing human cartilage in-vivo applying high resolution non-invasive SWI at UHF. The phase reconstruction methods VRC and COMPOSER yield phase images suitable for the SWI of the knee. Both deoxyhemoglobin containing vessels and layers of epiphyseal cartilage could be visualized with scanning times below 5 min. This opens the possibility to identify and analyze disorders of the growing cartilage at an early stage^{13,14}.

Acknowledgements

This study was supported by funds of the Oesterreichische Nationalbank (Oesterreichische Nationalbank, Anniversary Fund, project number: 16213).

References

1. Tóth, F. et al. Histological confirmation and biological significance of cartilage canals demonstrated using high field MRI in swine at predilection sites of osteochondrosis. *J. Orthop. Res.* 31, 2006–2012 (2013).
2. Nissi, M. J. et al. Susceptibility weighted imaging of cartilage canals in porcine epiphyseal growth cartilage ex vivo and in vivo. *Magn. Reson. Med.* 71, 2197–2205 (2014).
3. Nissi, M. J., Tóth, F., Wang, L., Carlson, C. S. & Ellermann, J. M. Improved Visualization of Cartilage Canals Using Quantitative Susceptibility Mapping. *PLOS ONE* 10, e0132167 (2015).
4. Tóth, F. et al. Novel Application of Magnetic Resonance Imaging Demonstrates Characteristic Differences in Vasculature at Predilection Sites of Osteochondritis Dissecans. *Am. J. Sports Med.* 43, 2522–2527 (2015).
5. Gründer, W. MRI assessment of cartilage ultrastructure. *NMR Biomed.* 19, 855–876 (2006).
6. Robinson, S. D. et al. Combining phase images from array coils using a short echo time reference scan (COMPOSER). *Magn. Reson. Med.* (2015). doi:10.1002/mrm.26093
7. Hammond, K. E. et al. Development of a robust method for generating 7.0 T multichannel phase images of the brain with application to normal volunteers and patients with neurological diseases. *NeuroImage* 39, 1682–1692 (2008).
8. Parker, D. L., Payne, A., Todd, N. & Hadley, J. R. Phase reconstruction from multiple coil data using a virtual reference coil. *Magn. Reson. Med.* 72, 563–569 (2014).
9. Koopmans, P. J., Manniesing, R., Niessen, W. J., Viergever, M. A. & Barth, M. MR venography of the human brain using susceptibility weighted imaging at very high field strength. *Magn. Reson. Mater. Phys. Biol. Med.* 21, 149 (2008).
10. Bollmann, S., Zimmer, F., O'Brien, K., Vegh, V. & Barth, M. When to perform channel combination in 7 Tesla quantitative susceptibility mapping? in Proceedings of the Annual Meeting of Human Brain Mapping Meeting # 1858, (2015).
11. Noll, D. C., Nishimura, D. G. & Macovski, A. Homodyne detection in magnetic resonance imaging. *IEEE Trans. Med. Imaging* 10, 154–163 (1991).
12. Robinson, S., Grabner, G., Witoszynskyj, S. & Trattnig, S. Combining phase images from multi-channel RF coils using 3D phase offset maps derived from a dual-echo scan. *Magn. Reson. Med.* 65, 1638–1648 (2011).
13. Ytrehus, B., Carlson, C. S. & Ekman, S. Etiology and Pathogenesis of Osteochondrosis. *Vet. Pathol. Online* 44, 429–448 (2007). 14. Carlson, C. S., Hillel, H. D. & Meuten, D. J. Degeneration of Cartilage Canal Vessels Associated With Lesions of Osteochondrosis in Swine. *Vet. Pathol. Online* 26, 47–54 (1989).

Figures

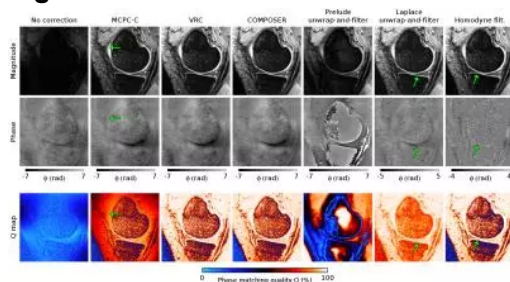


Figure 1: Comparison of phase combination approaches on the oldest subject, that with thinnest cartilage (C6, age 15) representing the most challenging case. The magnitude (top row) and the phase (middle row) of the complex combined signal, as well as phase matching quality index, Q (bottom row) are presented for all methods considered. Arrows point to the locations of errors in phase described in the main text.

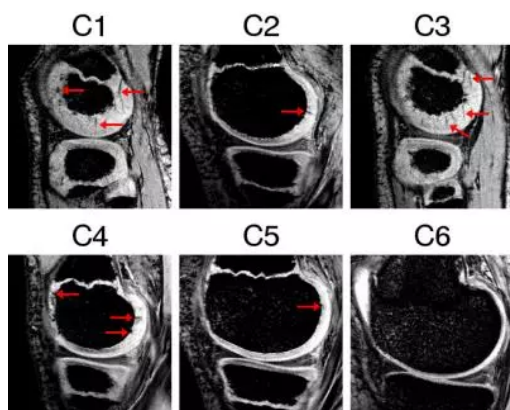


Figure 2: Examples of the appearance of cartilage channels in SWI. Arrows point to the most evident examples of veins. Subjects are illustrated in age order: the number of vessels generally reduced with age, with no apparent vasculature for the oldest subject C6 (age 15).

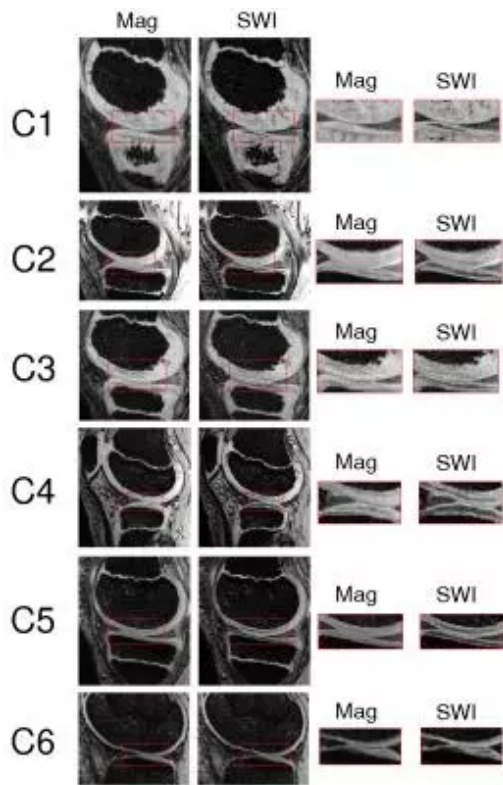


Figure 3: Examples of contrast in SWI appearing to correspond to layers of differing fiber orientation and not apparent in magnitude images.